CATHENA VALIDATION IN SUPPORT OF LARGE BREAK LOCA ANALYSIS

T.G. Beuthe and J.P. Mallory

Atomic Energy of Canada Limited
Whiteshell Laboratories
Pinawa, Manitoba, Canada R0E 1L0

ABSTRACT

An effort is currently underway to improve the validation of the CATHENA thermalhydraulics code for use in CANDU reactor safety analysis and licensing. As part of this work, a series of RD-12, RD-14, and RD-14M simulations were performed to help qualify CATHENA for large break loss-of-coolant accident analysis. This paper discusses modelled and experimental results from large break loss-of-coolant accident tests conducted in the RD-12, RD-14, and RD-14M test facilities and how they are used in the validation process.

1 INTRODUCTION

CATHENA is being validated using the industry wide phenomenology-based matrix approach to code validation [1]. This approach identifies the accident categories for reactor safety analysis, the primary phenomena in each category, and the experimental data that can be used to assess and validate the adequacy of the models in reproducing these phenomena. The information presented in this paper provides an overview of a portion of the work conducted to date in support of the use of CATHENA for large break Loss-Of-Coolant Accident (LOCA) analysis in CANDU® reactors. The primary phenomena of interest to large break LOCA analysis are identified by the industry wide phenomenology-based matrix. These include break discharge characteristics, coolant voiding, quench/rewet characteristics, and convective heat transfer. Data from the RD-12, RD-14, and RD-14M integrated test facilities were identified as being appropriate for validating these phenomena. Data from these facilities were also selected to demonstrate that scaling and multiple channel effects are captured by the code. CATHENA MOD-3.5b/Rev 0 simulations of experiments conducted in these facilities were performed on an HP-UX 9000/800 computer.

2 CATHENA

CATHENA (Canadian Algorithm for THErmalhydraulic Network Analysis) is a computer program developed by AECL at Whiteshell Laboratories (WL) primarily for the analysis of postulated LOCA events in CANDU reactors. CATHENA uses a transient, one-dimensional two-fluid representation of two-phase flow in piping networks. In the thermalhydraulic model, the liquid and vapour phases may have different pressures, velocities, and temperatures. The thermalhydraulic model consists of solving six partial differential equations for the conservation of mass, momentum, and energy for each phase. Interface mass, energy, and momentum transfer between the liquid and vapour phases are specified using constitutive relations obtained either from the literature or developed from separate-effects experiments.

The computer program uses a staggered-mesh, one-step, semi-implicit, finite-difference solution method, that is not transit time limited. The extensive wall heat transfer package can account for radial and circumferential

---

CANDU® is a registered trademark of Atomic Energy of Canada Limited (AECL).

conduction, solid-solid contact, thermal radiation, pressure tube deformation, and the zirconium-steam reaction. The heat transfer package is general and allows the connection of multiple wall surfaces to a single thermalhydraulic node. The CATHENA computer program also includes component models required for complete loop simulations such as pumps, valves, tanks, break discharges, separator models, and an extensive control system modelling capability. A more complete description of the CATHENA thermalhydraulic computer program is provided in [2].

3 FACILITY DESCRIPTIONS

Experiments have been performed in the RD-12, RD-14, and RD-14M experimental facilities to investigate large break loss-of-coolant accidents in CANDU reactors. Tests from these facilities were chosen to demonstrate CATHENA's ability to predict break discharge characteristics, coolant voiding, quench/rewet characteristics, and convective heat transfer for a variety of reactor-like facilities of various scales operated at reactor typical conditions.

3.1 RD-12 Facility

As shown schematically in Figure 1, the RD-12 facility was a small scale pressurized-water loop containing the essential features of a CANDU reactor arranged in a figure-of-eight configuration. It was designed to operate at reactor typical conditions (i.e., pressure, temperature). The test selected had a single channel per pass configuration with each channel containing a 3.9 m-long, 7-element electrically heated bundle or Fuel Element Simulator (FES) in the Test Section. The RD-12 large break blowdown test used in this work was selected to be comparable to an RD-14 test to demonstrate the CATHENA computer code can account for the effects of scale. Of the available RD-12 tests in which the Emergency Core Coolant (ECC) system was used the chosen test had the longest period at full power after break initiation and hence had the highest channel temperatures.

3.2 RD-14 Facility

As shown schematically in Figure 2, the RD-14 facility was also a pressurized-water loop with the essential features similar to the primary heat transport loop of a typical CANDU reactor. This facility was full vertical reactor scale, with full size feeders and channels. It had a single channel per pass configuration with each pass containing a 6-m long, 37-element electrically heated bundle. It was designed to operate at reactor-typical conditions (i.e., pressure, temperature, flowrate, mass flux). The RD-14 large break blowdown test data was selected because the loop was full vertical scale and contained full size feeders and channels (see reference [3] for further details). The RD-14 and RD-12 large break LOCA tests were conducted under similar conditions. They were chosen to demonstrate the code could account for the effects of scale. The tests used in this work were selected to cover the range of break sizes and break locations investigated in the facility. Results from a representative test are shown in this paper.

3.3 RD-14M Facility

As shown schematically in Figure 3, the RD-14M facility is a pressurized-water loop with the essential features similar to the primary heat transport loop of a typical CANDU reactor. The facility is full vertical reactor scale with the channel inlet and outlet feeder piping arrangements designed to represent the Darlington Nuclear Generating Station feeders. The loop has a multiple (5) channel per pass configuration with each channel containing a 6-m long, 7-element electrically heated bundle (see reference [4] for further details). The

RD-14M facility was designed to operate at reactor-typical conditions (i.e., pressure, temperature, mass flux, transit time). The RD-14M large break blowdown test data was selected because the loop was full vertical scale and contained a multiple channel per pass configuration. Comparison of RD-14 and RD-14M test data addresses the issue of multiple channel effects. The RD-14M large break blowdown tests used in this work were also selected to cover the range of break sizes and break locations investigated in the facility. Results from a representative test are shown in this paper.

4 RD-12 IDEALIZATION

The CATHENA idealization used to simulate the RD-12 facility primary-side, secondary-side and ECC systems is shown in Figures 4, 5 and 6 respectively. The idealization had 409 thermalhydraulic nodes, 412 links, 154 wall heat transfer models and 568 fluid-wall heat transfer surfaces.

The primary-side idealization, shown in Figure 4, consisted of the RD-12 primary-side piping connecting the headers, test sections containing the FES, steam generators, and primary pumps. Only the portion of the surge tank line up to the surge tank isolation valve was included, since the surge tank was isolated prior to initiation of the break. The surge tank was modelled as a pressure boundary condition. The heat transfer models in GENHTP (GENeralized Heat Transfer Package) were used to account for the heat transfer from the primary fluid to the pipe walls, from pipe walls to the environment, and from the steam generator tubes to the secondary-side fluid. Pipe radii (inner and outer) were used to define the metal mass and heat transfer area in contact with the primary fluid. Heat losses to the environment were accounted for. The thermal properties used for the piping materials as well as the material in the 7-element fuel element simulators were obtained from CATHENA's internally stored temperature dependent properties or derived from standard references.

The secondary-side idealization of the RD-12 test facility is shown in Figure 5. This idealization included the steam generators and that part of the feedwater line from the thermocouple location measuring feedwater temperature to the steam generator feedwater inlets. Portions of the feedwater line upstream of this location were represented by flow and enthalpy boundary conditions extracted from the experimental data.

The CATHENA idealization of the RD-12 ECC system is shown in Figure 6. System Control models were used to open the ECC isolation valves at the same time as in the experiment. Time-varying pressure boundary conditions, extracted from experimental data, were used to model the high-pressure ECC tank pressure response.

5 RD-12 SIMULATION RESULTS

Once a steady state had been established, a CATHENA simulation of the RD-12 experiment was conducted. Figures 7, 8, 9 and 10 show representative simulated and measured header pressures, ECC flows, and test section outlet void fractions and FES pin temperatures respectively for test B8223.

5.1 RD-12 Primary System Pressure and ECC Flowrate

As shown in Figure 7, Header 1 rapidly depressurizes starting at 10 s (break initiation time) as a result of the break at header 3. The depressurization curves of headers 1, 2, and 4 are similar to each other, whereas the depressurization of header 3 is more rapid, owing to the break at this location. As illustrated in Figures 7 and 8 the simulation results closely follow the experimental results.

The ability to accurately predict header pressures can be used as an indirect validation of the ability of CATHENA to predict break discharge characteristics. Break discharge rates were not measured in the RD-12 facility. However, good agreement between simulated and experimental break discharge rates can be inferred from agreement between simulated and measured system pressures, since system pressure is strongly affected by the discharge rate. In the RD-12 test under examination here, critical saturated, two phase flow, as well as subcritical liquid flow occurred at the break. As illustrated in Figure 7, the modelled header pressures were in agreement with the experimental measurements throughout the transient. Consequently, it may be inferred that the break discharge characteristics were captured by the CATHENA simulation.

5.2 RD-12 Void and FES Temperature

Figure 9 shows the measured and simulated void history at the outlet of Test Section 1 (TS1). For comparative purposes, Figure 10 shows the experimental and modelled outlet top pin FES temperature histories. It should also be noted that although the FES temperature measurements were taken inside the test section, the void fractions were measured downstream in the piping attached to the test section. Thus, the measured void does not necessarily reflect the void occurring in the channel.

As illustrated in Figures 9 and 10, as the system depressurized, voiding occurred in TS1, and the top FES temperature rapidly increased shortly after the break was initiated at 10 s. The FES temperatures reached about 750 °C by 20 s. By 50 s, the FES temperature had reduced to 200 °C as the power to the FES was reduced to decay power, and the FES was cooled by the two-phase flow occurring in the channel. The upper FES began to heat up once again at 90 s under the influence of the decay power and the reduced flow in the channel. ECC entered at the channel inlet at about 180 s and channel refill was completed by 225 s.

Figure 9 shows that the timing for the onset of void in TS1 was well simulated by CATHENA and the void fractions in the initial stages of the blowdown were also captured well. However, the modelled TS1 top pin temperatures exceed the experimental values in the first 150 s of the simulation (see Figure 10). This overestimation results from an underestimation of the film boiling heat transfer rates for some conditions. While this is undesirable, the results are considered conservative. Refilling and final quenching of the channel occurred earlier than in the experiment.

The FES temperature in TS2 (not shown) decreased monotonically after the break was initiated as flowrates through TS2 increased due to the proximity of the broken header downstream (see Figure 1). CATHENA correctly demonstrated that dryout did not occur in TS2 and that the FES remained well cooled despite continued high void at the outlet after ECC entered the channel.

6 RD-14 IDEALIZATION

The CATHENA idealization of the RD-14 facility primary side, secondary side and ECC systems is shown in Figures 11, 12, and 13 respectively. The complete RD-14 idealization had 274 thermalhydraulic nodes, 279 links, 101 wall heat transfer models and 647 fluid-wall heat transfer surfaces.

The primary-side idealization, shown in Figure 11, consisted of the RD-14 primary-side piping connecting the headers, heated sections, steam generators, and primary pumps. Only that portion of the surge tank line up to the surge tank isolation valve was included, since the surge tank was isolated prior to the initiation of the break.

GENHTP models were used to account for the heat transfer from the primary fluid to the pipe walls, from pipe walls to the environment, and from the steam generator tubes to the secondary side fluid. The heat transfer

coefficients applied to the outside of the piping, to simulate heat losses to the environment, were derived from RD-14 heat loss tests. The thermal properties used for the piping materials were obtained from CATHENA's internally stored temperature dependent properties.

The secondary-side idealization of the RD-14 test facility is shown in Figure 12. This idealization included the steam generators up to the steam nozzle and that part of the feedwater line from the thermocouple location measuring the feedwater temperature to the steam generator feedwater inlets. Portions of the feedwater line upstream of this location were represented by flow and enthalpy boundary conditions. The secondary-side steam generator outlet pressures were modelled using pressure boundary conditions obtained from the experimental boiler steam drum pressures.

The CATHENA idealization of the RD-14 ECC system is shown in Figure 13. It included provision for both the high-pressure tank and low-pressure (pumped) injection modes used in the RD-14 facility.

7 RD-14 SIMULATION RESULTS

Initially, steady state conditions were established for each RD-14 CATHENA simulation to ensure that an energy balance between all metal surfaces and the fluid had been obtained. Steady state FES temperatures were used to validate the ability of CATHENA to predict liquid convective heat transfer for a variety of flowrates and powers. Simulation results were compared to the initial 10 s of steady state data taken at the beginning of each test. The results show that CATHENA is able to capture single phase liquid heat transfer with acceptable accuracy.

Once steady states had been established, CATHENA simulations of a number of different RD-14 large inlet and outlet header break tests were conducted. Figures 14, 15, 16, and 17 show simulated and measured header pressures, ECC flows, test section outlet void fractions, and test section outlet pin temperatures for outlet header break test B8711. In all cases, the blowdown and high-pressure ECC injection phases of the test are shown.

7.1 RD-14 Primary System Pressure and ECC Flowrate

As illustrated in Figures 14 and 15 the header pressure for the B8711 test shows rapid depressurization down to the ECC injection pressure after opening the break. The primary pressure continued to decline after the onset of ECC, reaching about 2 MPa(a) by about 45 s. Between 45 and 90 s, the pressure and ECC flowrates stabilized. With the termination of high-pressure ECC between 80 and 90 s and the onset of low-pressure pumped injection, ECC flowrates decreased and the primary pressure declined to less than 1 MPa(a). The CATHENA simulation results show that the header pressures and ECC flowrates were well predicted. While some discrepancies between measured and simulated pressures and ECC flowrates did appear, they tended to be of short duration.

As discussed earlier for the RD-12 simulation, the ability of CATHENA to predict break discharge characteristics may be inferred from its ability to predict header pressures since the primary system pressure is largely impacted by the discharge rate. Break discharge rates were not measured in the RD-14 facility, but the good agreement between experimental and simulated primary system pressures such as those shown in Figure 14 indicate that CATHENA was able to predict the discharge rate. The discharged coolant in the RD-14 tests experienced both critical and subcritical flow at saturated single-phase, two-phase, as well as highly non-equilibrium fluid conditions. Results from the other tests in the CATHENA validation showed that CATHENA correctly captured the effect of break size on break discharge characteristics.

7.2 RD-14 Void and FES Temperature

Figures 16 and 17 show measured and simulated void fractions, and top and bottom FES temperature histories in the middle of TS1 respectively. The void fraction was measured in the piping attached to the heated section, whereas the FES temperatures were taken inside the heated section. Therefore, the void fraction measurements do not necessarily reflect the void fraction behaviour in the test section.

The B8711 experiment was a large outlet header break test in which forward flow increased on break initiation in TS2 (not shown), and void briefly appeared before ECC entered TS2 at about 35 s. Quenching and refilling of TS2 was complete by 40 s. In TS1, forward flow initially continued and rapid voiding occurred at the outlet, as shown in Figure 16. By 30 s the the test section was almost completely voided and remained so until ECC began refilling the channel at about 55 s. As shown in Figure 16 the CATHENA simulated void fraction behaviour in TS1 is in acceptable agreement with measured results. The simulated void in the unbroken pass was also well captured. The channel void fraction data shown in Figure 16 was also used to validate the ability of CATHENA to capture coolant voiding. Simulated and experimental channel inlet and outlet pressures, voids, and FES temperatures were examined in the early portion of the blowdown (the first 25 s after the break). Results of this work showed that the CATHENA calculated parameters are in good agreement with the experimental results, leading to the conclusion that CATHENA is able to accurately capture coolant voiding.

Figure 17 shows the simulated and measured top and bottom FES temperature histories at the middle of TS1. In test B8711, no significant temperature excursion was seen in either channel. TS1 showed a small temperature excursion at the initiation of the break which was quickly quenched since the high-quality, high-velocity flow through the channel was sufficient to maintain good cooling. The CATHENA results tend to overestimate the brief temperature excursion at the beginning of the blowdown phase of the experiment. Since CATHENA tends to underestimate the film boiling heat transfer rates, the simulation results did not indicate quenching of the FES until the arrival of ECC later in the test. However, FES temperature excursions were correctly simulated not to occur in TS2.

8 RD-14M IDEALIZATION

The CATHENA idealization of the RD-14M facility primary side, secondary side and ECC systems used to simulate test B9013 is shown in Figures 18, 12, and 19 respectively. The complete RD-14M idealization had 518 thermalhydraulic nodes, 532 links, and 178 wall heat transfer models.

The RD-14M primary side idealization consisted of all piping connecting the headers, test sections, steam generators, pumps and surge tank as shown in Figure 18. The volume, length, flow area and elevation change of each CATHENA pipe component resembled, as closely as possible, the RD-14M test facility. The break occurred at inlet header 8.

GENHTP models were used to simulate all solid components in contact with the fluid. They were also used to account for the heat transfer from all solid components in contact with the fluid and the heat transfer from the primary fluid to the pipe walls to the environment, or in the case of the steam generator tubes, to the secondary side. Pipe radii were used in defining the metal mass and heat transfer area in contact with the primary fluid. Heat losses to the environment were also accounted for.

The secondary side model used to simulate the test is shown in Figure 12. The RD-14M and RD-14 secondary side models are identical since the same steam generators were used in both experiments.

The CATHENA idealization of the ECC configuration used in test B9013 is shown in Figure 19. This idealization includes provisions for both the high pressure ECC phase where water is injected from a pressurized tank (CANDU-6 configuration) and the low pressure ECC phase where water is injected using a pump. In the high pressure ECC phase, time varying pressure boundary conditions extracted from experimental data were used to model the high pressure ECC tank since unknown quantities of nitrogen gas were injected into the ECC tank in an attempt to maintain a constant tank pressure.

9 RD-14M SIMULATION RESULTS

Initially, steady state conditions were established for each RD-14M CATHENA simulation to ensure that an energy balance between all metal surfaces and the fluid had been achieved. As with the RD-14 simulations, RD-14M simulations of the steady state were used to help validate CATHENA simulations of convective heat transfer for a variety of flowrates and powers under single phase conditions. The RD-14M results showed that CATHENA is able to simulate single phase liquid heat transfer with acceptable accuracy.

Once steady states had been established, CATHENA simulations of several RD-14M inlet header break experiments with different sized breaks were conducted. Figures 20, through 22 show representative measured and simulated results from one of the inlet header break cases (B9013). All plots show the blowdown phase, the high pressure ECC injection phase and part of the low pressure pumped ECC injection phase.

9.1 RD-14M Primary System Pressure and ECC Flowrate

Figures 20 and 21 show the measured and calculated pressure for header 8 (the broken header) and the corresponding header ECC flowrates respectively. The experimental header pressure shows the rapid depressurization down to the injection pressure within a few seconds after the initiation of the break. The primary pressure continued to decline after the onset of high pressure ECC, reaching about 1.0 MPa(a) by 60 s. With the termination of the high pressure ECC phase and the onset of the low pressure pumped injection at about 225 s, ECC flowrates decline. CATHENA header pressures show good agreement with the experimental results. As illustrated in Figure 21, the distribution of ECC flowrates to each individual header was not as well modelled, but the results were considered acceptable.

As with the RD-12 and RD-14 results, the good agreement between the modelled and experimental RD-14M header pressures indicates that CATHENA simulates the critical and subcritical single-phase and two-phase discharge conditions, at various break sizes, with acceptable accuracy.

9.2 RD-14M Void and FES Temperature

Figures 22 and 23 show measured and calculated void fractions, and FES temperature histories of an upper elevation pin respectively at the outlet of Test Section 13 . Void fraction was measured in the piping attached to the test section while the FES temperature measurements were taken within the test section. Therefore, the void fraction measurements do not necessarily reflect the void fraction behaviour in the test section.

As illustrated in Figure 22, rapid and nearly complete voiding of Test Section 13 took place on initiation of the break. Similar results occurred in all test sections in the pass in which the break occurred. Refilling of these test sections occurred from the outlet end. As shown in Figure 23 the FES temperature excursions in the test sections within the broken pass immediately began upon initiation of the break as flow in these channels dropped significantly to very low values. The FES temperatures initially increased quickly and then slowed as

the channel power was reduced to decay levels beginning at about 12 s. Shortly after the onset of the high pressure ECC injection phase, quenching began as ECC water entered these channels.

Test sections in the unbroken pass (no example shown) experienced rapid voiding immediately after the initiation of the break, but only at the outlet end since flow remained forward through these sections during this time. Voiding at the inlet occurred later in the test. No significant temperature excursions were recorded in the unbroken pass as channel flows remained high enough to maintain adequate cooling of the FES. The CATHENA simulation shows similar results.

The CATHENA calculated void fraction behaviour of all the heated sections in both the broken and unbroken pass are in good agreement with the measured results. CATHENA correctly calculated that rapid and near complete voiding at the inlet and outlet test sections in the broken pass occurred upon the initiation of the break. As with the RD-14 results, the RD-14M void fraction data from the broken pass was used to validate the ability of CATHENA to predict coolant voiding. Results showed that CATHENA calculated parameters are in good agreement with the experimental results, leading to the conclusion that CATHENA is able to accurately capture coolant voiding. CATHENA correctly demonstrated that only the outlet of the test sections in the unbroken pass experienced rapid voiding at the break initiation.

In general the FES temperatures also showed acceptable agreement with the measured results. CATHENA indicated that large FES temperature excursions occurred in the test sections in the broken pass immediately after the break. However, peak FES temperatures tended to be overestimated. CATHENA correctly calculated that the FES in the channels in the unbroken pass did not experience any significant temperature excursions after the initiation of the break as sufficient flow through these channels was present to maintain adequate cooling.

As illustrated in Figure 23, the FES temperatures at the outlet of the channels in the broken pass quenched at about the same time as indicated by the void fraction in Figures 22. It should be noted that quenching in some channels may not have been caused by the arrival of ECC water, but rather by a flow generated in the channels at the onset of high pressure ECC injection. Overall, quenching of the channels in the broken pass was in acceptable agreement with the measured results, indicating CATHENA correctly captured the parameters affecting the quench/rewet characteristics.

10 SUMMARY AND CONCLUSIONS

CATHENA is currently being validated using the phenomenology-based validation matrix approach. This approach identified that data from RD-12, RD-14, and RD-14M was suitable for validating a number of primary phenomena of the large break accident category. CATHENA simulations of RD-12, RD-14, and RD-14M tests have helped show that break discharge characteristics, coolant voiding, quench/rewet characteristics, and convective heat transfer phenomena are captured with acceptable accuracy by CATHENA. Use of data from all three facilities have also helped to address scaling and multiple channel effects.

ACKNOWLEDGEMENTS

Construction and operation of the RD-14 and RD-14M facilities was funded by the CANDU Owners Group.

REFERENCES

1. E.O. Moeck, J.C. Luxat, M.A. Petrilli, and P.D. Thompson, "Status of Validation Matrices for CANDU Power Plants", Proceedings of the 18th Annual Conference of the Canadian Nuclear Society, June 8–11, 1997.
2. B.N. Hanna, "CATHENA: A thermalhydraulic code for CANDU analysis", Nuclear Engineering & Design, 180 (1998) 113–131.
3. P.J. Ingham, G.R. McGee, and V.S. Krishnan, "LOCA Assessment Experiments in a Full-Elevation, CANDU-Typical Test Facility", Nuclear Engineering and Design, 122 (1990) 401–412.
4. A.J. Melnyk, P.J. Ingham, and T.V. Murray, "Critical Break Experiments in the RD-14M Thermalhydraulic Test Facility", Proceedings of the 16th Annual CNS Simulation Symposium, St. John, New Brunswick, August 26–27, 1991.

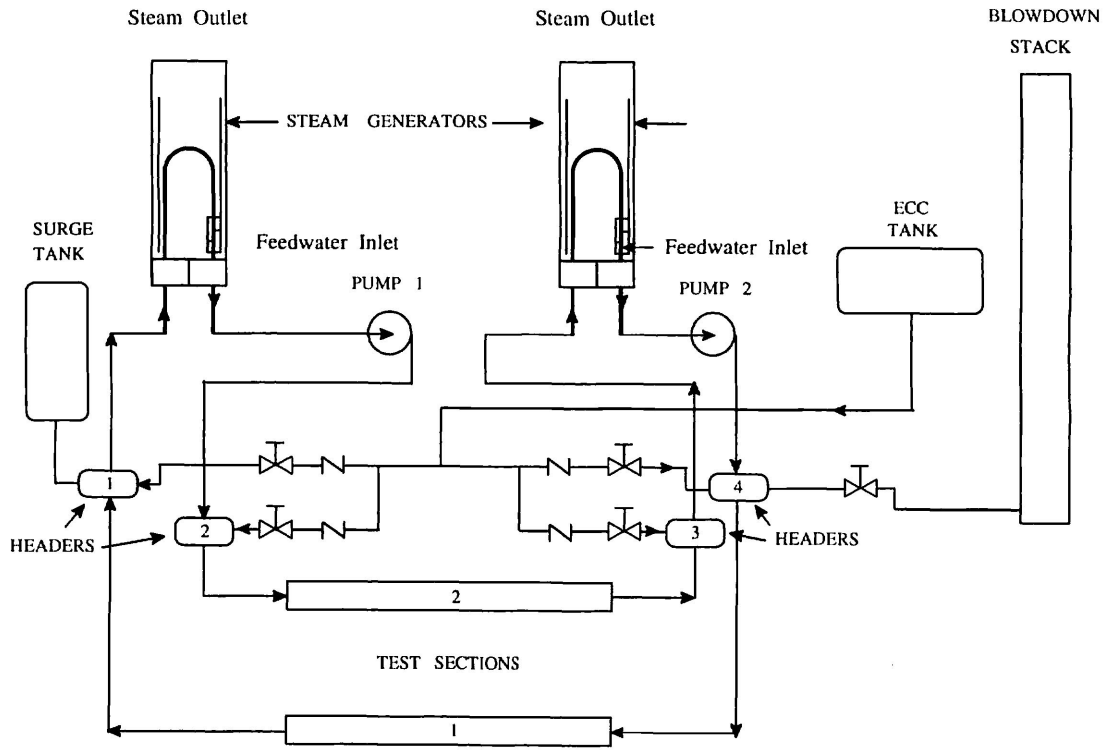

FIGURE 1: Schematic of the RD-12 Test Facility

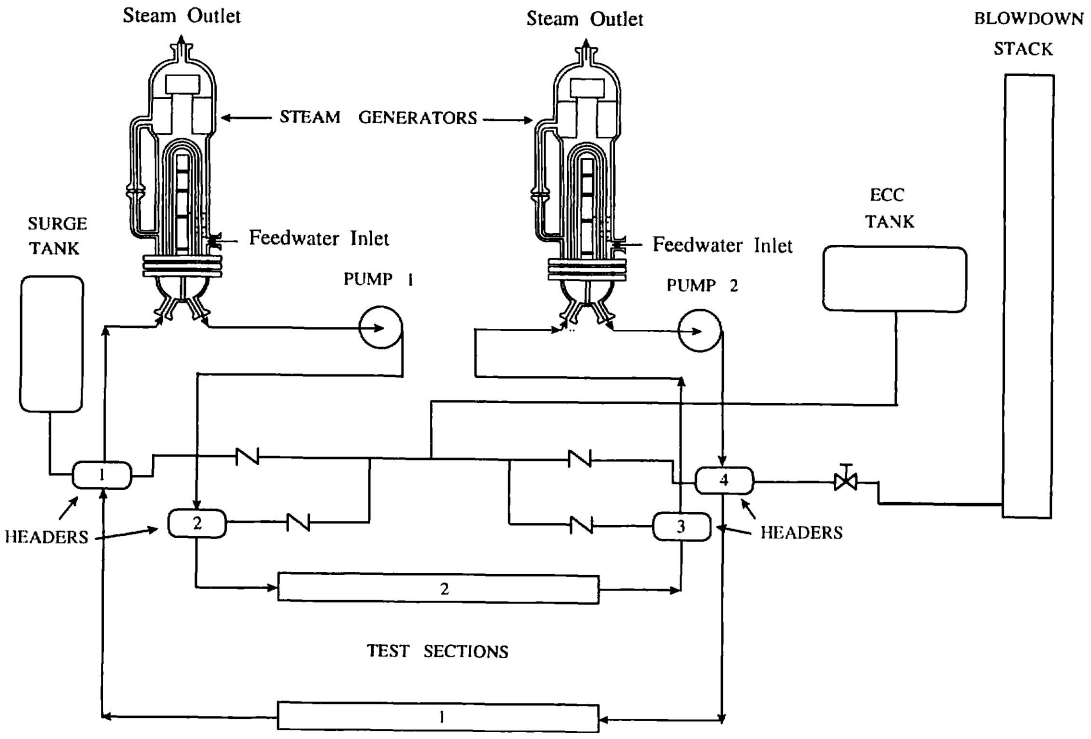

FIGURE 2: Schematic of the RD-14 Test Facility

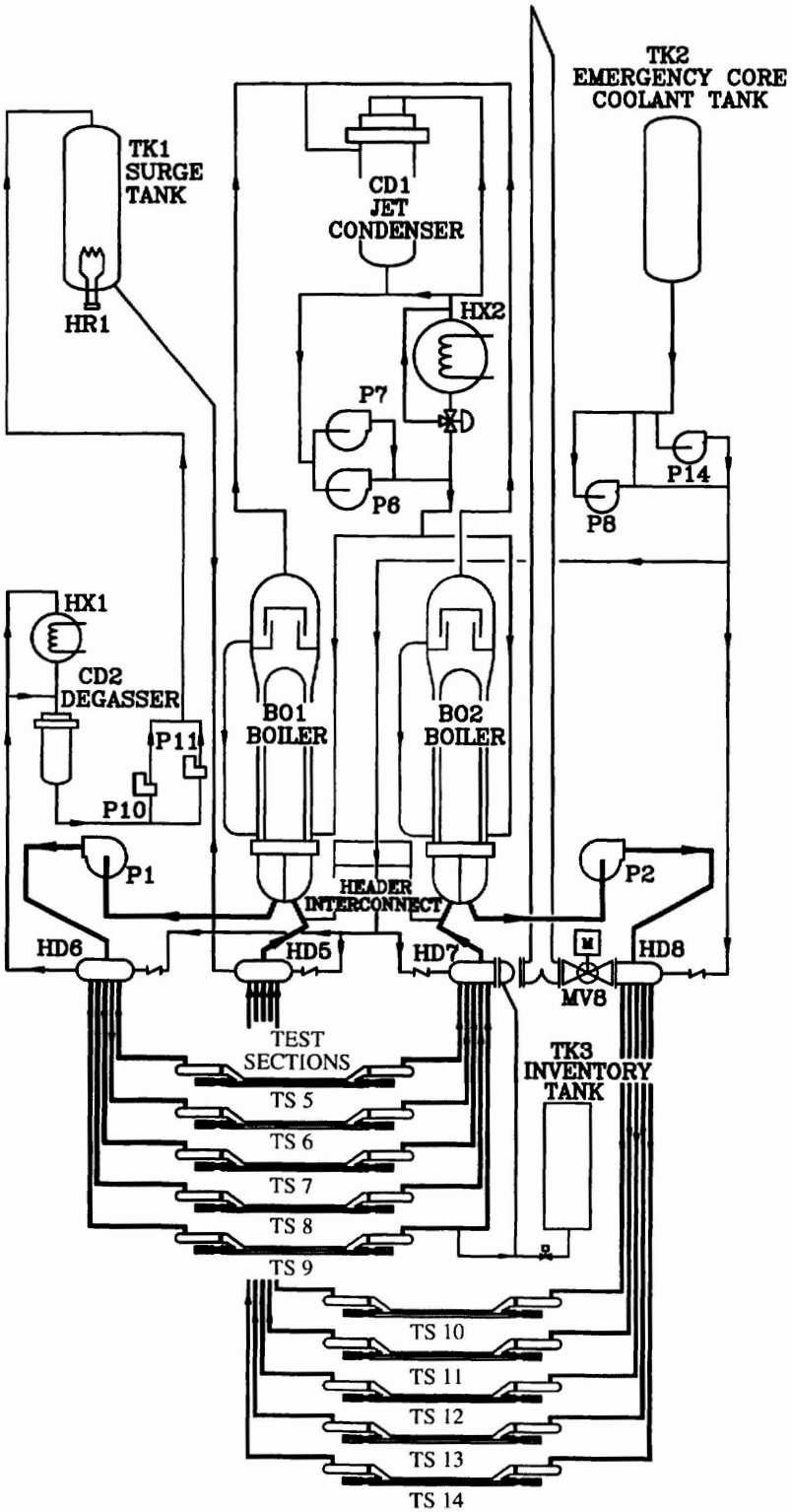

FIGURE 3: Schematic of the RD-14M Test Facility

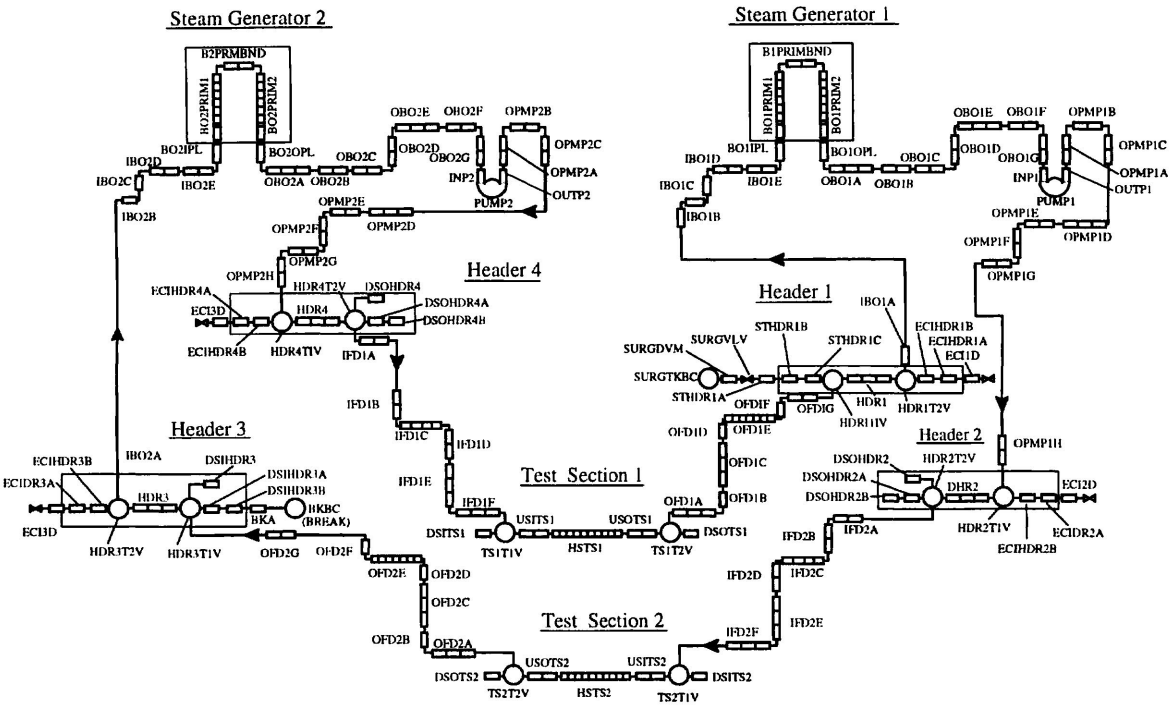

FIGURE 4: Thermalhydraulic Representation of RD-12 Primary Side

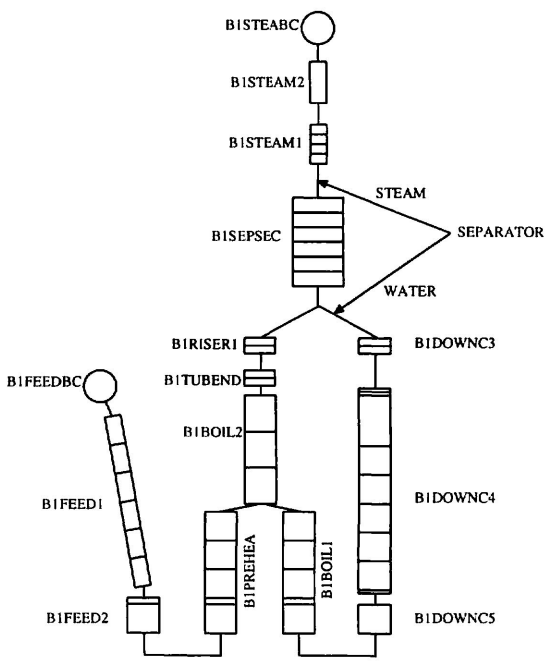

FIGURE 5: Thermalhydraulic Representation of RD-12 Secondary Side

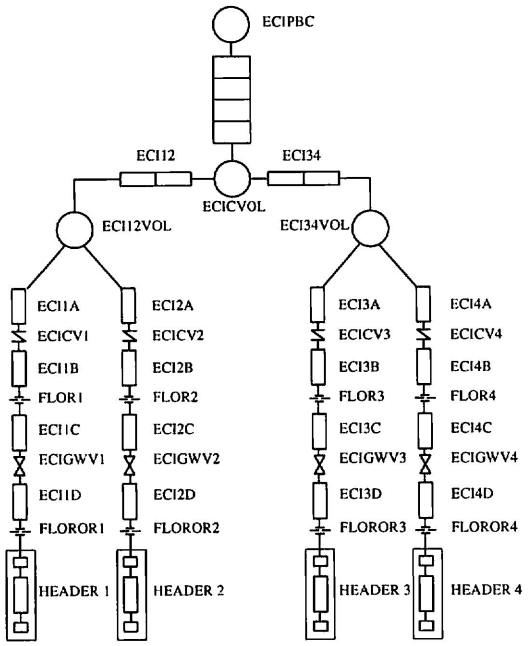

FIGURE 6: Thermalhydraulic Representation of RD-12 ECC System

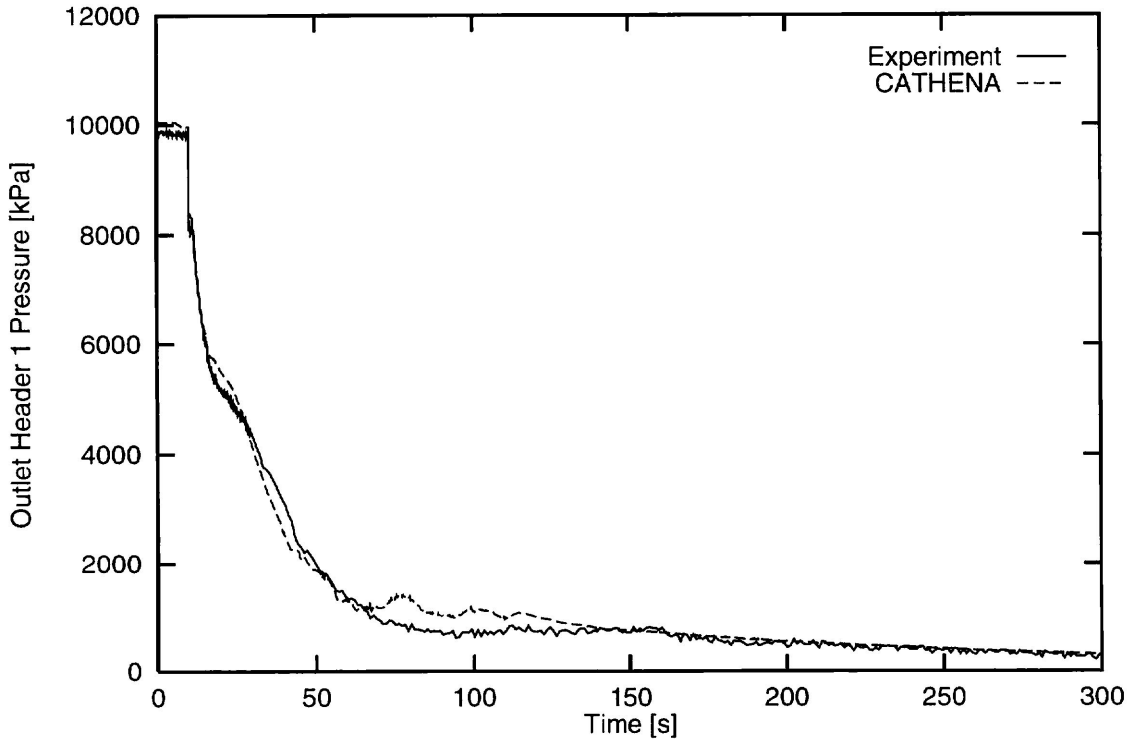

FIGURE 7: RD-12 Outlet Header 1 Pressure for test B8223.

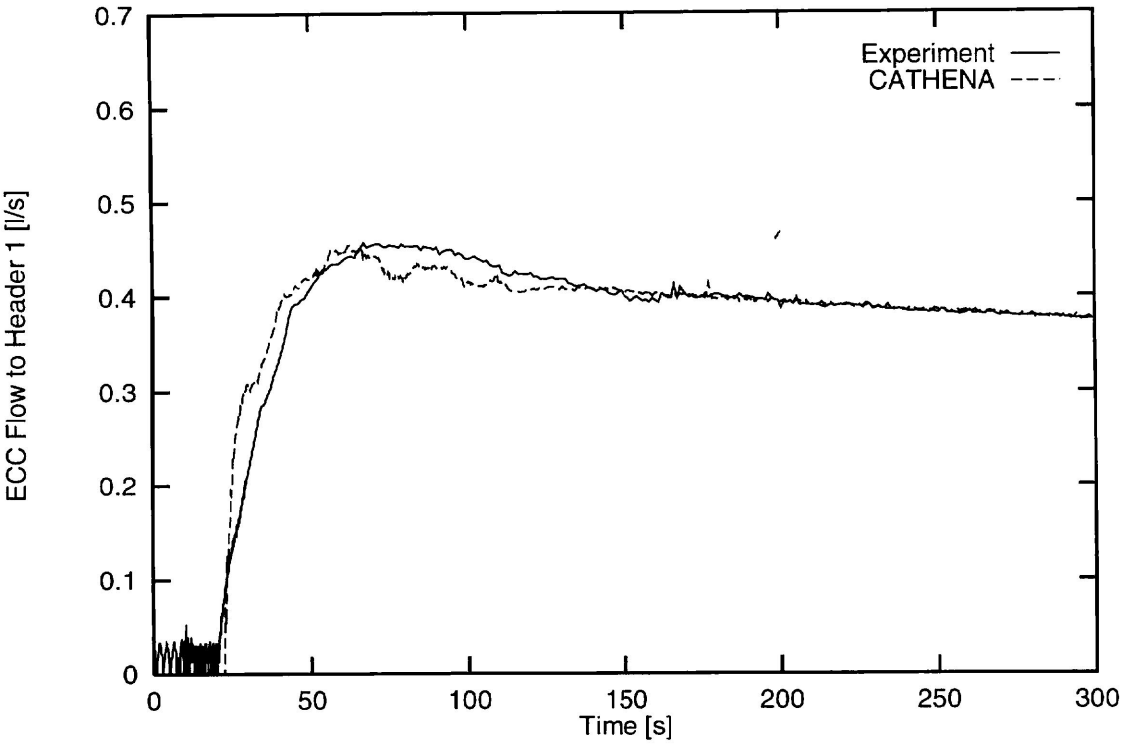

FIGURE 8: RD-12 Outlet Header 1 ECC Flow for test B8223.

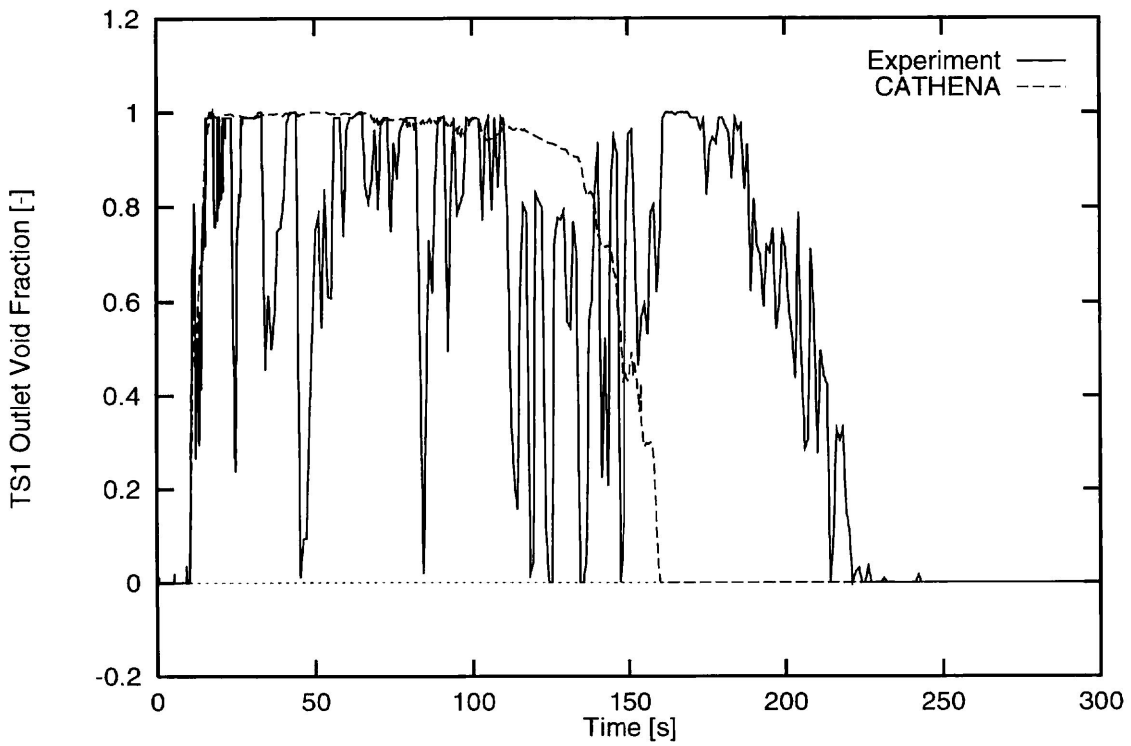

FIGURE 9: RD-12 TS1 Outlet Void Fraction for test B8223.

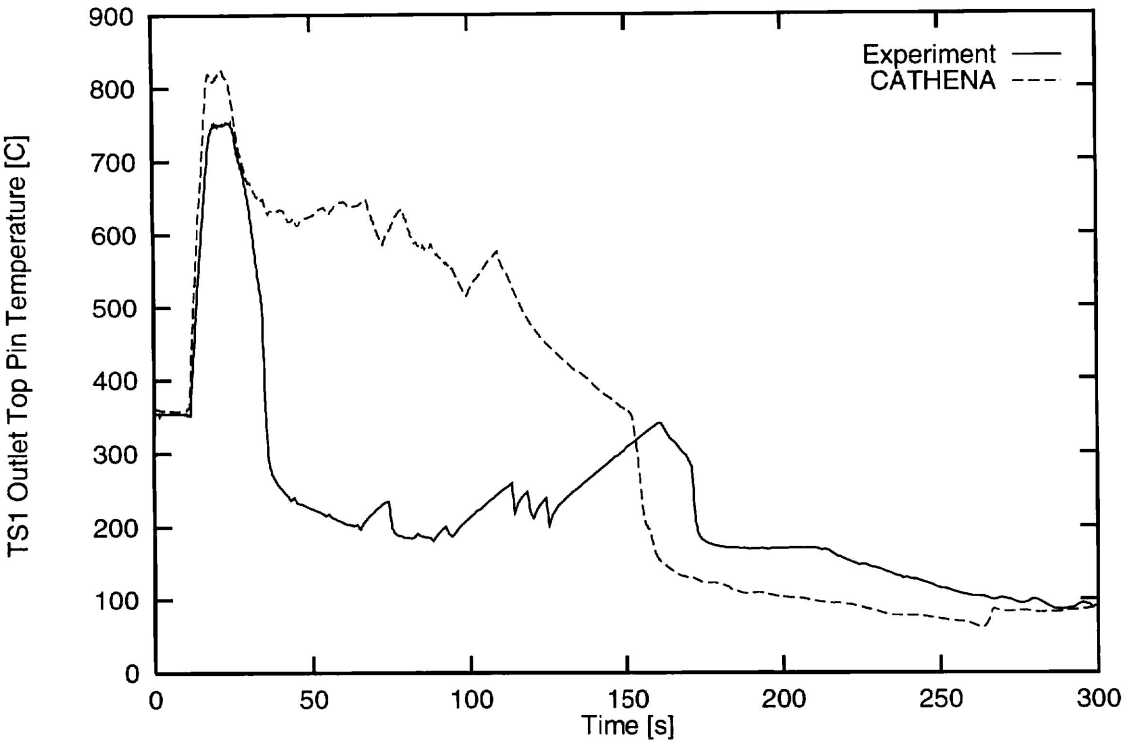

FIGURE 10: RD-12 TS1 Outlet Top Pin Temperature for test B8223.

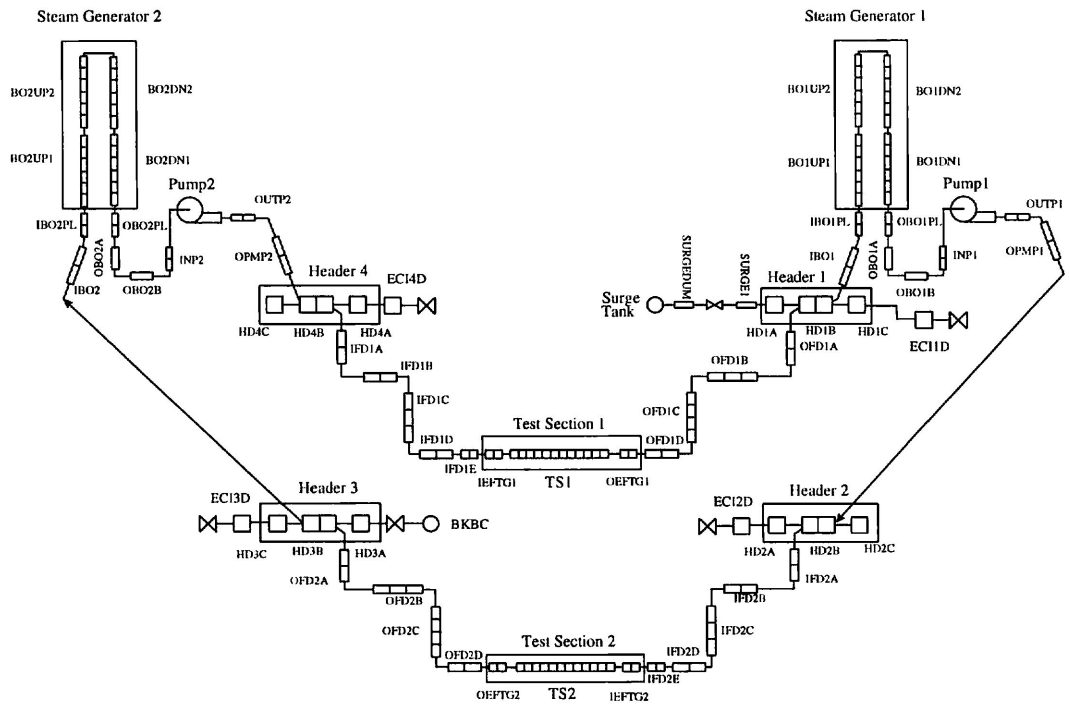

FIGURE 11: Thermalhydraulic Representation of RD-14 Primary Side

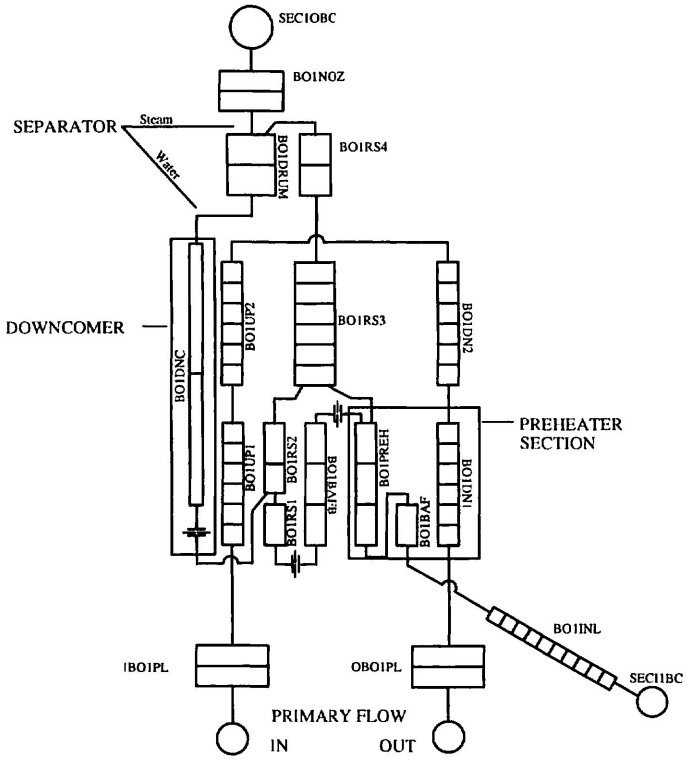

FIGURE 12: Thermalhydraulic Representation of RD-14 and RD-14M Secondary Side

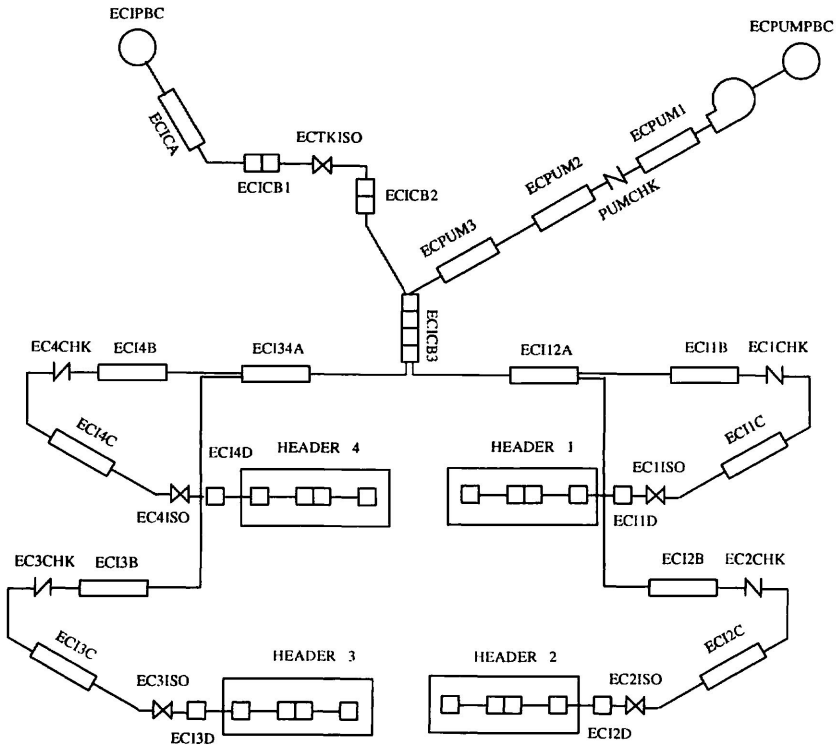

FIGURE 13: Thermalhydraulic Representation of RD-14 ECC System

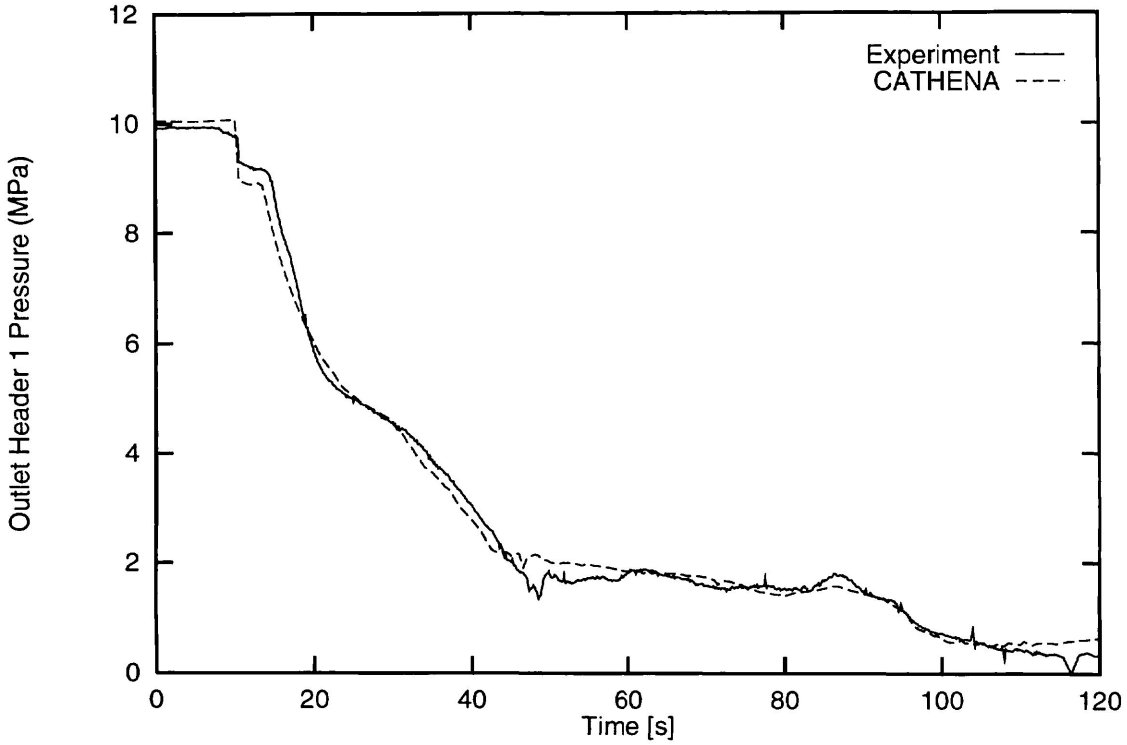

FIGURE 14: RD-14 Outlet Header 1 Pressure for Test B8711.

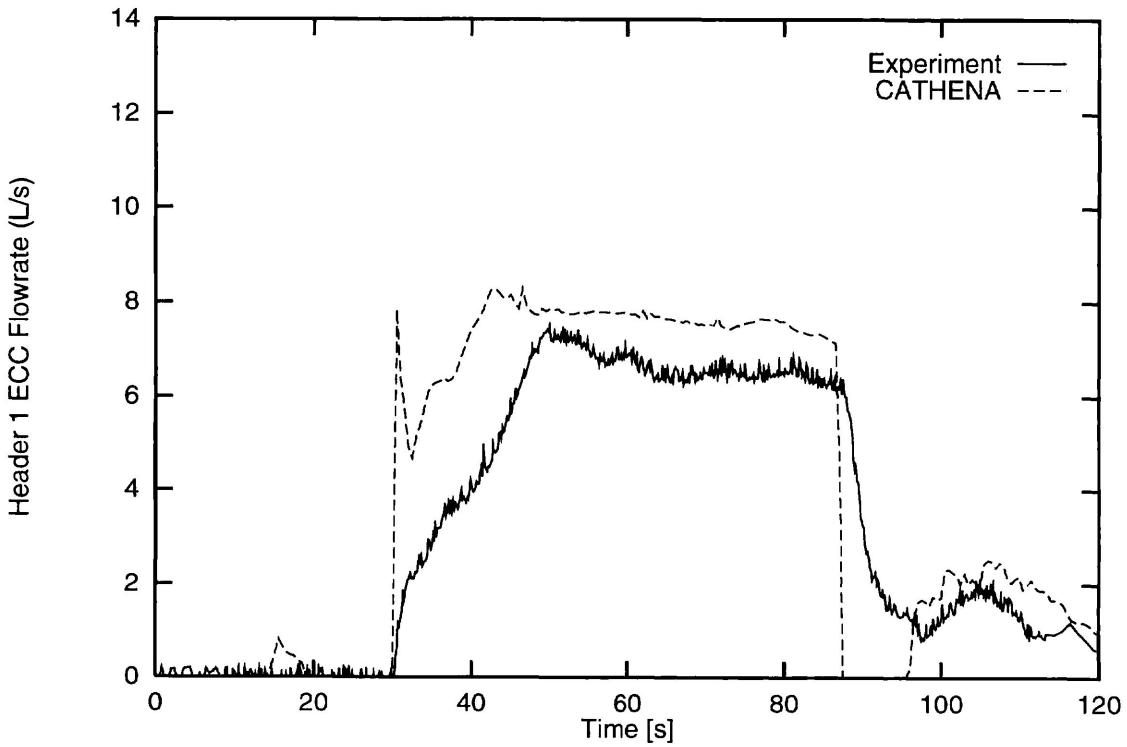

FIGURE 15: RD-14 Outlet Header 1 ECC Flow for Test B8711.

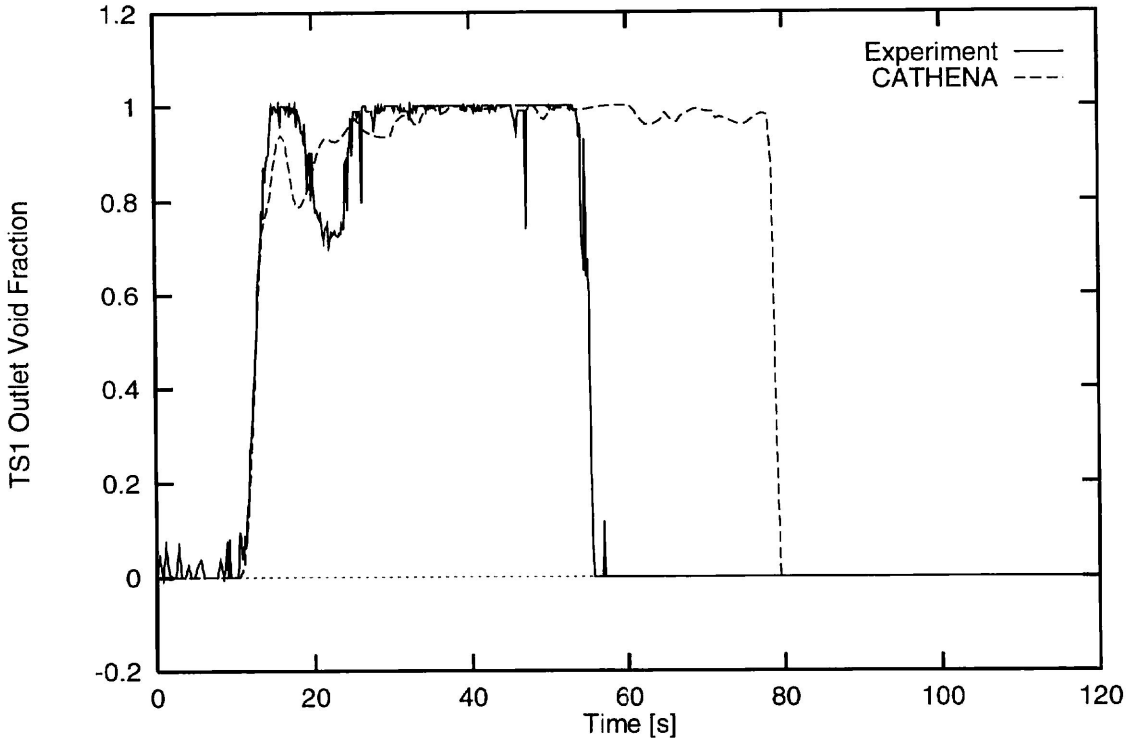

FIGURE 16: RD-14 TS1 Outlet Void Fraction for Test B8711.

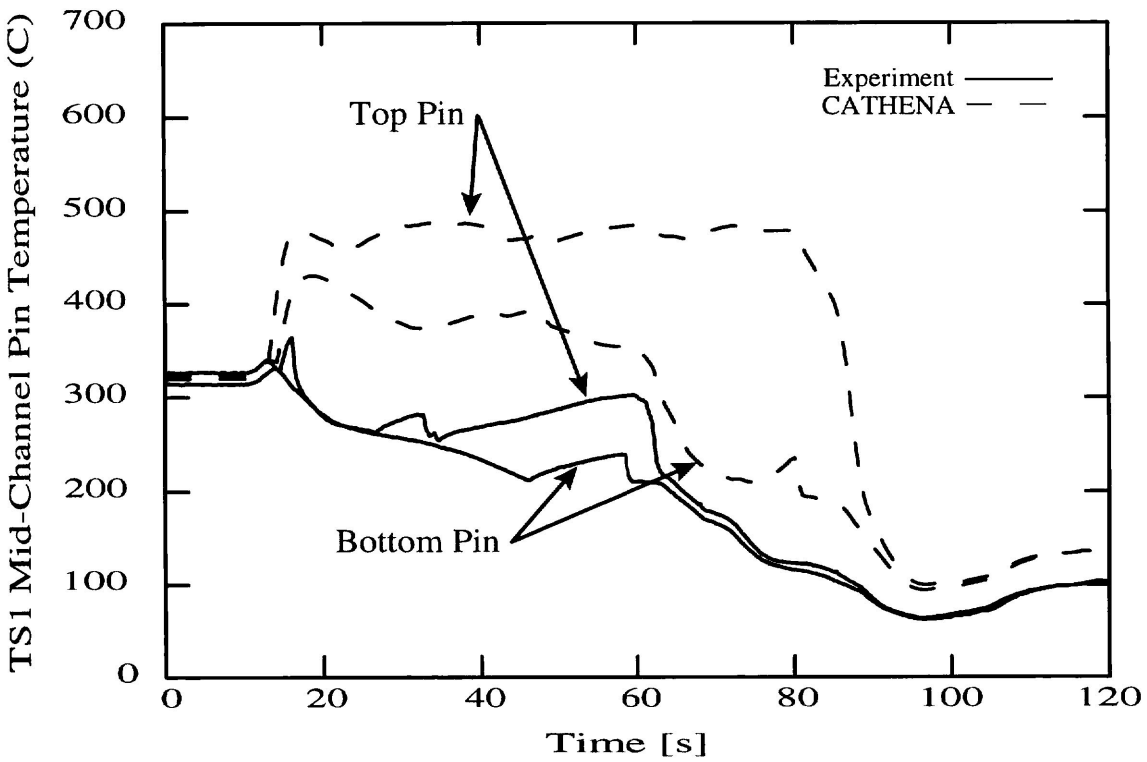

FIGURE 17: RD-14 TS1 Temperature for Test B8711.

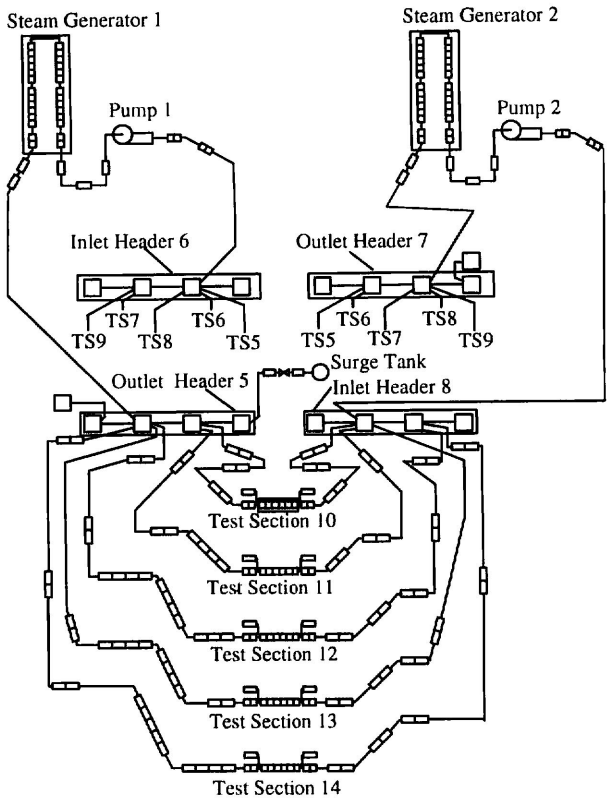

FIGURE 18: Thermalhydraulic Representation of RD-14M Primary Side

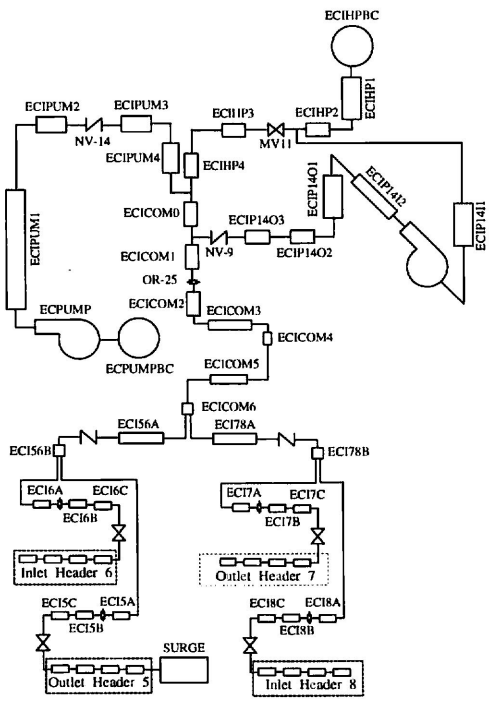

FIGURE 19: Thermalhydraulic Representation of RD-14M ECC System

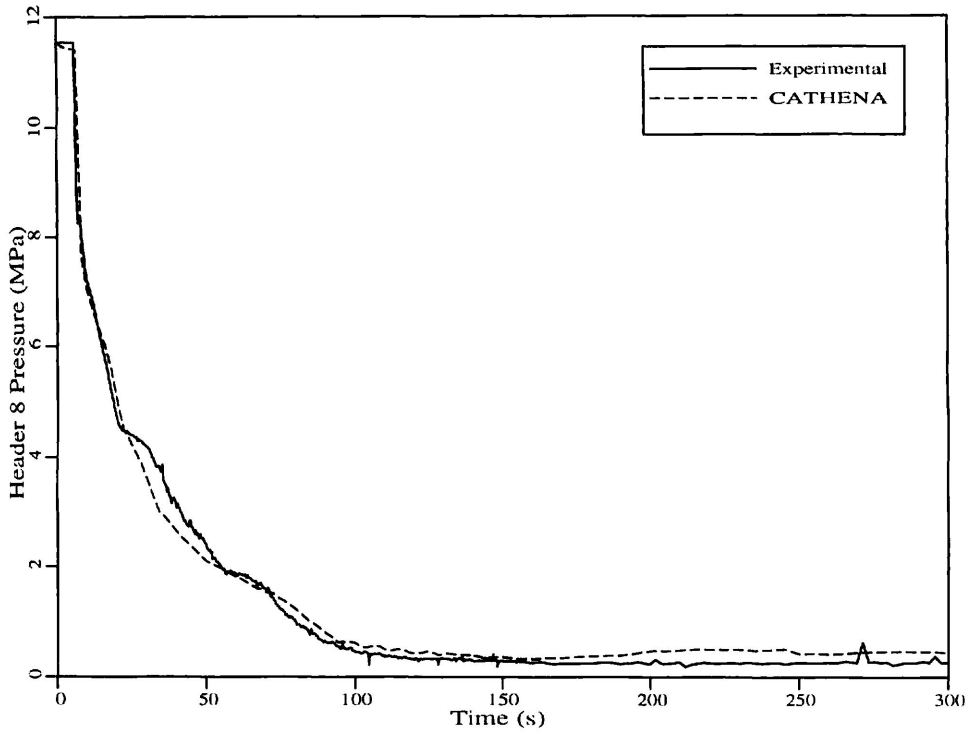

FIGURE 20: RD-14M Inlet Header 8 (Broken Header) Pressure for Test B9013

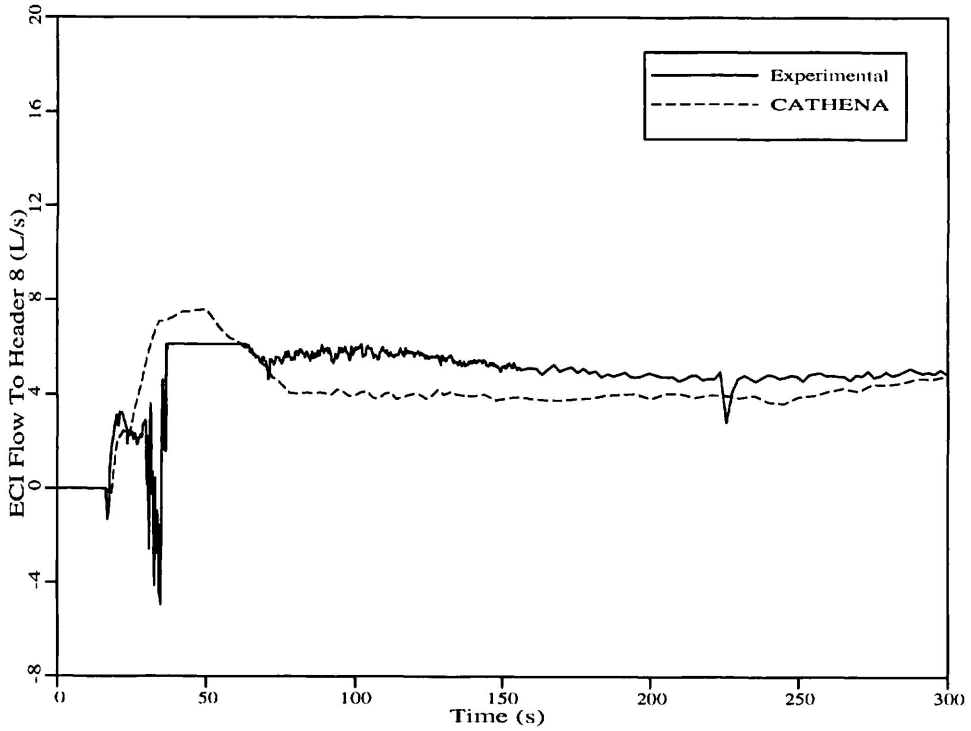

FIGURE 21: RD-14M Inlet Header 8 (Broken Header) ECC Flow for Test B9013

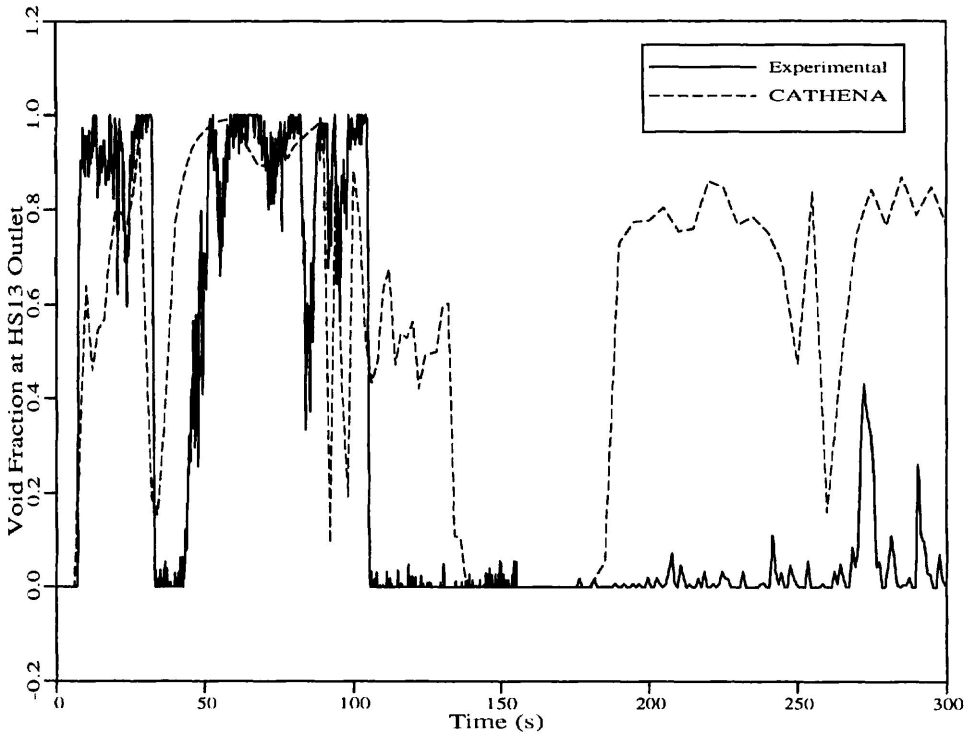

FIGURE 22: RD-14M Test Section 13 Outlet Void Fraction for Test B9013.

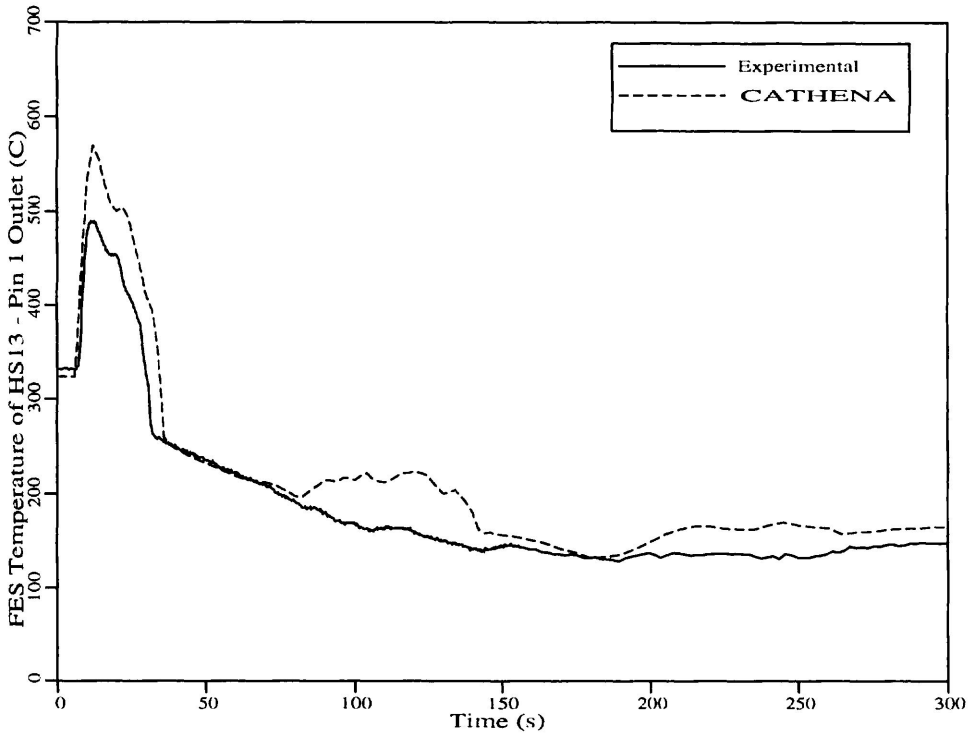

FIGURE 23: RD-14M Test Section 13 Outlet Top Pin Temperature for Test B9013.